

Odorant Receptor Map in the Mouse Olfactory Bulb: *in vivo* Sensitivity and Specificity of Receptor-defined Glomeruli

Yuki Oka, Sayako Katada, Masayo Omura, Makiko Suwa, Yoshihiro Yoshihara, and Kazushige Touhara

Figure S1. Expression and projection pattern of mOR-EG transgene

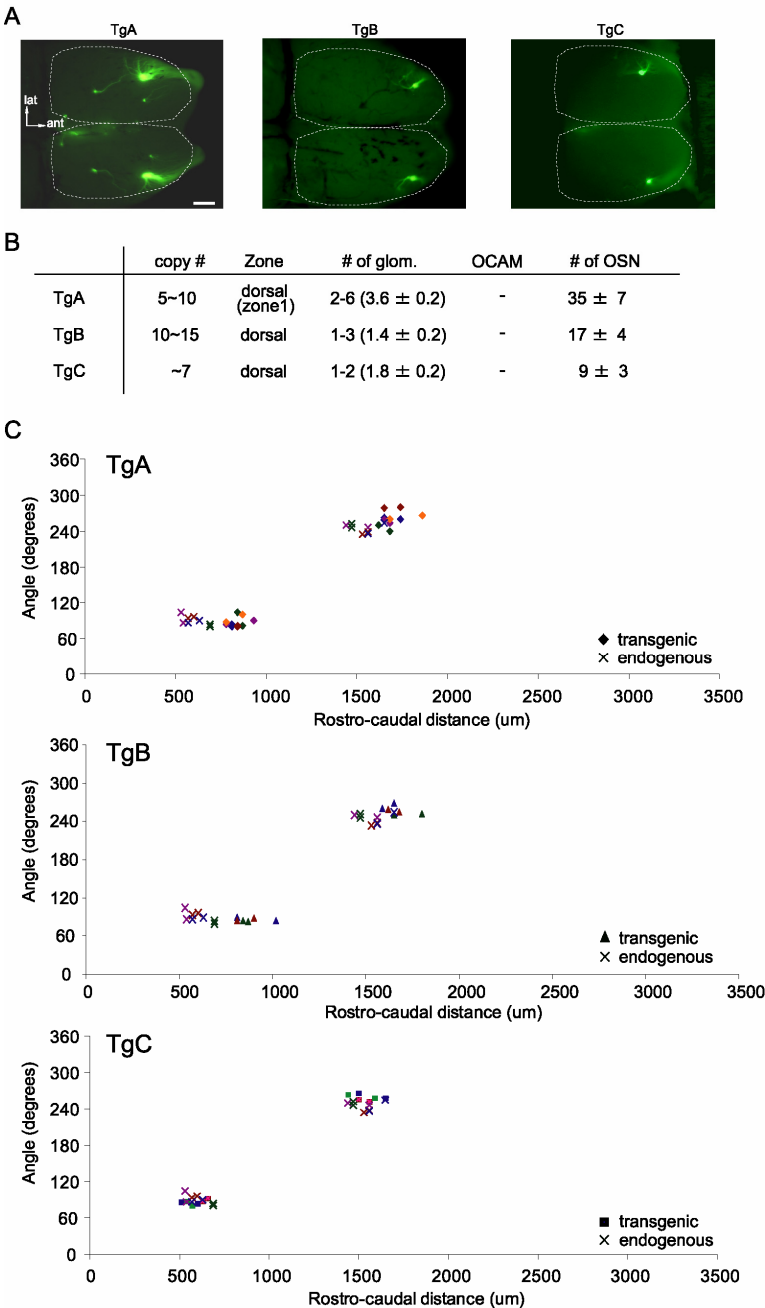
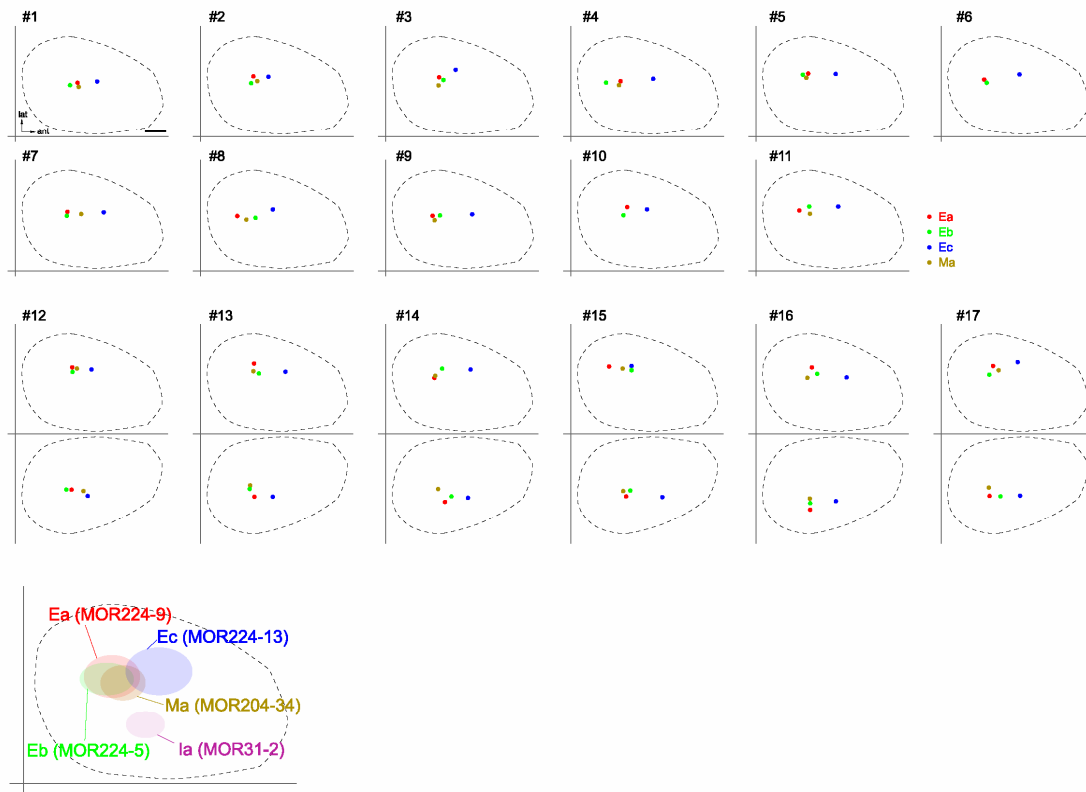


Figure S1. Expression and projection pattern of mOR-EG transgene. A, Dorsal view of the left and right OB (dotted line) of transgenic mice from the TgA (left), TgB (mid), and TgC (right). GFP signals are visible in the mOR-EG glomerulus. ant, anterior; lat, lateral. Scale bar, 500 μ m. B, Summary of expression pattern of the mOR-EG transgene. # of *glom.* indicates the number of GFP-positive glomeruli per bulb, counted by sectioning the OB, and the averaged numbers of glomeruli are shown in parenthesis (n = 14, 10, and 12 for TgA, TgB and TgC respectively). # of *OSN* indicates the number of GFP-positive OSNs in a 20- μ m section of the OE (average \pm S.E.). C, Positional relationship between transgenic and endogenous mOR-EG glomeruli. In all lines, the transgenic-derived GFP glomerulus was located closely posterior to the endogenous mOR-EG glomerulus. For the TgA, B, and C transgenic lines, each glomerular position was determined and represented as described previously (Schaefer et al., 2001). Glomeruli from the same animal are indicated by use of the same color. mOR-EG antibody was utilized to locate the endogenous mOR-EG glomerulus.

Figure S2. Location of OR-defined glomeruli in different animals

A



B

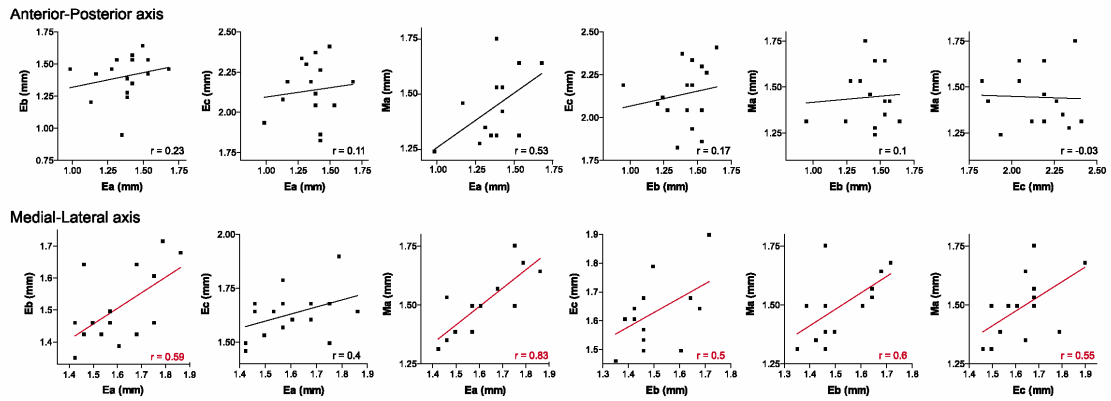
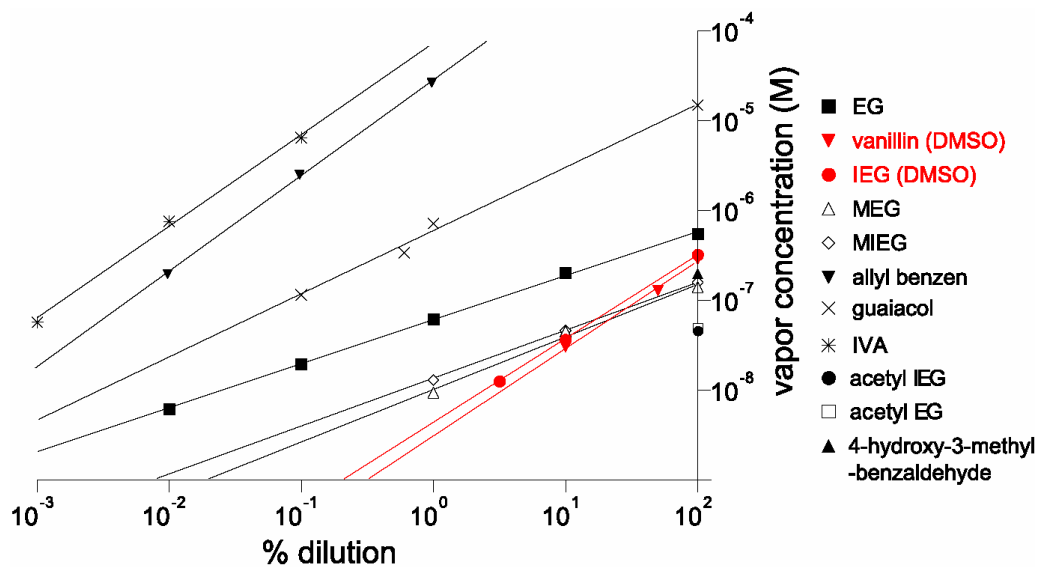


Figure S2. Location of OR-defined glomeruli in different animals. A, Glom. Ea, Eb, Ec, and Ma are shown with red, green, blue, and brown dots, respectively. The coordinates of each glomerulus were calculated as described in the Experimental Procedures. #1 to #11 (upper row) show the location of the glomerulus in the left OB of different animals (upper). #12 to #17 (middle row) show the bilateral location of glomeruli in different animals based on the Ca^{2+} -response map from both sides of the OB. The results from #12 to #15 are shown in Figure 6. The drawing at the bottom of the panel summarizes and represents each glomerular domain. B, Positional correlation between glomeruli. The positional correlation of each pair of glomeruli was calculated for both the anterior-posterior and the medial-lateral axis. The correlation coefficient (r) is indicated in each graph, and pairs of glomeruli showing a positive correlation are shown with red lines.

Figure S3. Vapor concentration of odorants



odorants	theoretical conc.	practical conc. (α)	exponent (β)
EG	559 (nM)	551	0.49
vanillin	104	290	0.96
IEG	279	320	0.94
MEG	1463	139	0.59
MIEG	592	157	0.54
allyl benzen	-	-	1.06
guaiacol	9630	14937	0.71
IVA	-	-	1.03
acetyl IEG	426	45	-
acetyl EG	174	49	-
4H3MBA	732	190	-

Figure S3. Vapor concentration of odorants. Log-log plot of vapor (M) vs. liquid (% v/v) concentration for various odorants. DMSO (IEG and vanillin; red line) or mineral oil (other odorants; black line) was used as the solvent. Results are the average of 2 to 4 measurements. Theoretical vapor concentrations were calculated using Advanced Chemistry Development software.

Saturated vapors of odorant solution in a 5-ml glass tube were sampled with a gas-tight syringe and loaded into an absorption tube. To measure the saturated vapor concentration, odorant solutions were used at least 3 h after dilution. Measurements were typically repeated three times, and the results from each experiment were averaged. The vapor concentration for each solvent can be calculated using the following equation (Cometto-Muniz et al., 2003):

$$[C_{\text{vap}}] = \alpha [C_{\text{liq}}]^{\beta}$$

where α is the vapor concentration of the pure substance, and exponent β is the slope from the log-log plot of vapor vs. liquid concentration. Both α and β are unique to each odorant, and are greatly affected by the type of solvent. We found that the vapor concentration is not necessarily proportional to the rate of odorant dilution. Therefore, we calculated exponent β by measuring the vapor concentration for each dilution step and then determining the corresponding dilution rate. We found that for some odorants, the vapor concentration was not simply proportional to the dilution ratio (Fried et al., 2002; Meister and Bonhoeffer, 2001). Odorant stimulation was delivered by placing a test tube filled with 3 ml of odorant solution within 1 mm of mouse nasal cavity for 3 or 5 s (for Ca^{2+} or intrinsic imaging, respectively).

Table S1. OR genes identified by retrograde dye labeling and degenerate PCR

la (9/17)	Ma (11/14)	Ea (13/34)	Eb (11/34)	Ec (6/13)
MOR31-2 (9)	MOR204-34 (8) MOR173-2 (1) MOR135-11 (1) MOR224-5 (1)	MOR224-9 (3) MOR188-3 (2) MOR171-28 (2) MOR171-12 (2) MOR161-2 (1) MOR127-1 (1) MOR123-1 (1) MOR204-23 (1) MOR202-34 (1) MOR204-13 (1)	MOR224-5 (3) MOR161-2 (3) MOR194-1 (2) MOR163-1 (1) MOR167-3 (1) MOR173-2 (1)	MOR224-13 (5) MOR171-7 (1)

Table S1. OR genes identified by retrograde dye labeling and degenerate PCR. For DiI-stained isolated OSNs, we first performed single cell RT-PCR using two sets of degenerate primers (see Materials and Methods). OR genes identified using degenerate primers are shown. A single OR gene was always amplified from a single OSN by degenerate primers, and the same OR gene was always amplified by different combinations of primers. Numbers in parenthesis indicate the population of cells from which OR genes were amplified. For example, for glom. Ma, we were able to amplify OR genes from 11 out of 14 DiI-positive OSNs using degenerate primers; MOR204-34 was amplified from 8 cells, MOR173-2, MOR135-11, and MOR224-5 were each amplified from one cell, and no OR gene was amplified from the remaining 3 cells. We then generated specific primers for the most frequently amplified ORs (one to four per glomerulus) and performed PCR on the original samples. For example, the MOR204-34 gene was amplified from an additional 2 out of the 3 remaining cells, resulting in a total of 10 out of 14 cells which were found to express MOR204-34, as shown in Figure 4A, left.

References

- Cometto-Muniz, J. E., Cain, W. S., and Abraham, M. H. (2003). Quantification of chemical vapors in chemosensory research. *Chem Senses* 28, 467-477.
- Fried, H. U., Fuss, S. H., and Korsching, S. I. (2002). Selective imaging of presynaptic activity in the mouse olfactory bulb shows concentration and structure dependence of odor responses in identified glomeruli. *Proc Natl Acad Sci U S A* 99, 3222-3227.
- Meister, M., and Bonhoeffer, T. (2001). Tuning and topography in an odor map on the rat olfactory bulb. *J Neurosci* 21, 1351-1360.
- Schaefer, M. L., Finger, T. E., and Restrepo, D. (2001). Variability of position of the P2 glomerulus within a map of the mouse olfactory bulb. *J Comp Neurol* 436, 351-362.